Baseline and Target Values for PV Forecasts: Toward Improved Solar Power Forecasting

Preprint

Jie Zhang[1], Bri-Mathias Hodge[1], Siyuan Lu[2], Hendrik F. Hamann[2], Brad Lehman[3], Joseph Simmons[4], Edwin Campos[5], and Venkat Banunarayanan[6]

[1] National Renewable Energy Laboratory
[2] IBM TJ Watson Research Center
[3] Northeastern University
[4] University of Arizona
[5] Argonne National Laboratory
[6] U.S. Department of Energy

Presented at the IEEE Power and Energy Society General Meeting
Denver, Colorado
July 26–30, 2015

NREL is a national laboratory of the U.S. Department of Energy
Office of Energy Efficiency & Renewable Energy
Operated by the Alliance for Sustainable Energy, LLC

This report is available at no cost from the National Renewable Energy Laboratory (NREL) at www.nrel.gov/publications.

Conference Paper
NREL/CP-5D00-63876
August 2015

Contract No. DE-AC36-08GO28308

NOTICE

This report is available at no cost from the National Renewable Energy Laboratory (NREL) at www.nrel.gov/publications.

Available electronically at SciTech Connect http:/www.osti.gov/scitech

Available for a processing fee to U.S. Department of Energy and its contractors, in paper, from:

U.S. Department of Energy
Office of Scientific and Technical Information
P.O. Box 62
Oak Ridge, TN 37831-0062
OSTI http://www.osti.gov
Phone: 865.576.8401
Fax: 865.576.5728
Email: reports@osti.gov

Available for sale to the public, in paper, from:

U.S. Department of Commerce
National Technical Information Service
5301 Shawnee Road
Alexandria, VA 22312
NTIS http://www.ntis.gov
Phone: 800.553.6847 or 703.605.6000
Fax: 703.605.6900
Email: orders@ntis.gov

Cover Photos by Dennis Schroeder: (left to right) NREL 26173, NREL 18302, NREL 19758, NREL 29642, NREL 19795.

NREL prints on paper that contains recycled content.

Baseline and Target Values for PV Forecasts: Toward Improved Solar Power Forecasting

Jie Zhang, Bri-Mathias Hodge
National Renewable Energy Laboratory
Golden, CO, USA

Siyuan Lu, Hendrik F. Hamann
IBM TJ Watson Research Center
Yorktown Heights, NY, USA

Brad Lehman
Northeastern University
Boston, MA, USA

Joseph Simmons
University of Arizona
Tucson, AZ, USA

Edwin Campos
Argonne National Laboratory
Lemont, IL, USA

Venkat Banunarayanan
U.S. Department of Energy
Washington, D.C., USA

***Abstract*—Accurate solar power forecasting allows utilities to get the most out of the solar resources on their systems. To truly measure the improvements that any new solar forecasting methods can provide, it is important to first develop (or determine) baseline and target solar forecasting at different spatial and temporal scales. This paper aims to develop baseline and target values for solar forecasting metrics. These were informed by close collaboration with utility and independent system operator partners. The baseline values are established based on state-of-the-art numerical weather prediction models and persistence models. The target values are determined based on the reduction in the amount of reserves that must be held to accommodate the uncertainty of solar power output.**

***Keywords*—grid integration; numerical weather prediction; operating reserve; ramp forecasting; solar power forecasting**

I. INTRODUCTION

The penetration of solar power in the electric grid is steadily rising, and the SunShot Vision Study reported that solar power could provide as much as 14% of U.S. electricity demand by 2030 and 27% by 2050 [1]. The increasing penetration of solar power has raised questions about how to best integrate variable renewable energy sources with the thermal power plants that dominate power production in the United States today. At high levels of solar energy penetration, solar power forecasting will become very important for electricity system operations, because it helps to reduce the uncertainty associated with the power output.

A. Baseline of Solar Forecasting

To truly measure the improvements that any new solar forecasting methods can provide, it is important to first assess the current state of the art in solar forecasting. A number of papers in the literature present global horizontal irradiance (GHI) forecast models for day-ahead and other similar timescale forecasts. Generally, a baseline model is used for comparison, which is selected from: (i) persistence models [2, 3]; (ii) numerical weather prediction (NWP) models without bias correction [4, 5]; and (iii) NWP models with bias correction [6, 7]. Most of the literature includes a comparison to persistence models in which the forecast 24 hours (or 48 hours, etc.) ahead is set to the measurement of irradiance from the day (or two, etc.) before. Even when comparing multiple models for different geographic locations to additional baselines, the persistence model is generally included as a reference.

This work was supported by the U.S. Department of Energy under Contract No. DE-AC36-08-GO28308 with the National Renewable Energy Laboratory. Valuable comments from the utility partners (ISO-New England, California-ISO, Green Mountain Power, and Tucson Electric Power) are gratefully acknowledged.

Relatively fewer papers in the literature present day-ahead baseline forecasts (or similar timescales) for solar power predictions; however, the approaches to solar power forecasting baselines seem to be similar to those for irradiance forecasts. Baseline models include (i) persistence models that set the day-ahead forecasted photovoltaic (PV) power equal to the measured PV power 24 hours before that time [8-10]; (ii) NWP + plane of array (POA) irradiance calculation + PV models [8-10]; and (iii) NWP with bias correction + POA irradiance calculation + PV models [8-10]. Essentially, baselines in the different PV power predictions for day-ahead forecasts always include a persistence model. They also seem to utilize one or more of the NWP forecast models.

B. Research Motivation and Objectives

Target values for the solar forecasting technology will establish the goals for improvements that are to be expected. Different strategies are used in power system operations at different timescales to ensure economic operations and reliability; thus, it is important to characterize solar forecasting at all timescales of interest. The baseline and target values will be made for different geographic and energy-market regions to evaluate the versatility of the technology.

The objective of this paper is to determine the baseline and target values for solar power forecasting metrics. A suite of generally applicable, value-based, and custom-designed metrics were adopted for evaluating solar forecasting for different scenarios. Section 2 presents the methodology for determining baseline and target values. Section 3 discusses the results of the California Independent System Operator (CAISO) case study. Concluding remarks and future work are given in the final section.

II. METHODOLOGY FOR DETERMINING BASELINE AND TARGET METRICS VALUES FOR SOLAR FORECASTING

Operations of power systems occur at different timescales that can be summarized, from longest to shortest, as unit commitment, load-following, economic dispatch, and regulation. To understand the impact of solar forecasts on solar power integration, it is important to characterize solar forecast errors at all timescales of interest. One of the objectives of this study is to determine the baseline and target solar forecasting metrics over a number of different timescales. Four solar forecast horizons are investigated: day-ahead (DA) forecasts, 4-hour-ahead (4HA) forecasts, 1-hour-ahead (1HA) forecasts, and 15-minute-ahead (15MA) forecasts.

A. Metrics for Assessing Solar Forecasting

A suite of generally applicable, value-based, and custom-designed metrics for solar forecasting for a comprehensive set of scenarios (different time horizons, geographic locations, applications, etc.) were developed in previous work by the authors [11]. The proposed solar forecasting metrics can be broadly divided into four categories: (i) statistical metrics for different time and geographic scales; (ii) uncertainty quantification and propagation metrics, (iii) ramp characterization metrics; and (iv) economic metrics. A brief description of the metrics is given in Table 1, and detailed information about each metric can be found in [11].

Table 1. PROPOSED METRICS FOR SOLAR POWER FORECASTING [11]

Type	Metric	Description/Comment
Statistical Metrics	Distribution of forecast errors	Provides a visualization of the full range of forecast errors and variability of solar forecasts at multiple temporal and spatial scales
	Pearson's Correlation coefficient	Linear correlation between forecasted and actual solar power
	Root mean square error (RMSE) and normalized root mean square error (NRMSE)	Suitable for evaluating the overall accuracy of the forecasts while penalizing large forecast errors in a square order
	Root mean quartic error (RMQE) and normalized root mean quartic error (NRMQE)	Suitable for evaluating the overall accuracy of the forecasts while penalizing large forecast errors in a quartic order
	Maximum absolute error (MaxAE)	Suitable for evaluating the largest forecast error
	Mean absolute error (MAE) and mean absolute percentage error (MAPE)	Suitable for evaluating uniform forecast errors
	Mean bias error (MBE)	Suitable for assessing forecast bias
	Kolmogorov–Smirnov test integral (KSI) or KSIPer	Evaluates the statistical similarity between the forecasted and actual solar power
	OVER or OVERPer	Characterizes the statistical similarity between the forecasted and actual solar power on large forecast errors
	Skewness	Measures the asymmetry of the distribution of forecast errors; a positive (or negative) skewness leads to an over-forecasting (or under-forecasting) tail
	Excess kurtosis	Measures the magnitude of the peak of the distribution of forecast errors; a positive (or negative) kurtosis value indicates a peaked (or flat) distribution, greater or less than that of the normal distribution
Uncertainty Quantification Metrics	Rényi entropy	Quantifies the uncertainty of a forecast; it can utilize all of the information present in the forecast error distributions
	Standard deviation	Quantifies the uncertainty of a forecast
Ramp Characterization	Swinging door algorithm	Extracts ramps in solar power output by identifying the start and end points of each ramp
Economic Metrics	95th percentile of forecast errors	Represents the amount of non-spinning reserves service held to compensate for solar power forecast errors

B. Methodology for Determining Baseline Values

From the temporal point of view, the simplest approach to estimate forecasting baselines is that of climatology. The climatology approach consists of using a constant long-term average value throughout the entire forecasting period; the average value is often used as a benchmark for the forecasting skill with minimal effort. However, we consider that the solar forecasting sector has surpassed this benchmark, and a better baseline approach is need.

Instead, we decided to use two other fundamental forecasting approaches: the model and the persistence approaches. The model approach corresponds to the use of products from NWP models, which rarely achieve useful skill at lead times smaller than a few hours because of the (spin-up) period they require to achieve numerical stability. The persistence approach (more specifically, Eulerian persistence) corresponds to using the persistence of the recent observations. This shows superior skill in the shorter forecasting periods and when atmospheric variability is smaller (e.g., dry climates, few clouds).

In general, the persistence forecasts show better skill than the model forecasts in the short term, whereas the model forecasts show better skill (than the persistence) after a few hours in the forecasting period [12]. Therefore, our baseline forecasts for 0- to 4-hour lead times use the persistence approach, whereas our day-ahead baseline forecasts use the model approach.

Given the aforementioned consideration, the overall methodology for establishing baseline values is summarized in Table 2. The establishment of baseline values for day-ahead forecasting for each of the metrics is based on a state-of-the-art weather model, specifically the North American Mesoscale Forecast System (NAM) [13], in combination with a streamer radiative transfer model (RTM) and the PV-Lib toolbox [14] for irradiance-to-power modeling. A modified persistence model is adopted for the 15MA, 1HA, and 4HA forecasts.

Table 2. OVERALL APPROACH TO ESTABLISHING BASELINES

Forecast Horizon	Weather Information	Irradiance Forecasts	Power Forecasts
15MA, 1HA, and 4HA	Persistence	Streamer RTM	Persistence of cloudiness
DA	NAM	Streamer RTM	PV-Lib or linear least square fit (if no PV specifications available)

1) Numerical Weather Predictions for DA Solar Forecasting

This day-ahead forecast uses NAM weather forecasting and a streamer RTM. The 5-km grid NAM forecast that runs at 06z daily is employed. Two NAM forecast windows, 0 to 23 hours ahead and 24 to 47 hours ahead, are used to derive solar irradiance forecasts for the two types of day-ahead (0 to 23 hours and 24 to 47 hours ahead) baseline values.

The vertical profiles (39 vertical levels) of pressure, temperature, geopotential height, humidity, cloud liquid water content, cloud ice content, and surface albedo are taken from the NAM forecast. The climatological monthly average of ozone concentration and aerosol optical depth are taken from the MODIS data set. Together these form the input for the streamer RTM [15], which solves the radiative transfer equation for the plane-parallel geometry using the spherical harmonic discrete ordinate method to calculate GHI and direct normal irradiance (DNI) at the Earth's surface. The GHI, DNI, ambient temperature (2 m above ground), and wind speed (10 m above ground) are then fed into an irradiance-to-power model to derive forecasted AC PV power. The irradiance-to-power model consists of two parts: (i) the PV modules are modeled using the CEC model, and (ii) the inverters are modeled using the Sandia National Laboratories model, both of which are implemented in PV-Lib [14].

2) Persistence for 15MA, 1HA, and 4HA Solar Forecasting

The 15MA, 1HA, and 4HA forecasts were synthesized using a persistence of cloudiness approach. In this method, the solar power index (*SPI*) is first calculated, which represents the ratio between actual power (*P*) and clear-sky power (P_{CS}). Then the solar forecast power is estimated by modifying the current power output by the expected change in clear-sky output. For the 1HA persistence of cloudiness approach, the forecast solar power at time *t+1* can be calculated as follows:

$$P(t+1) = P(t) + SPI(t) \times [P_{CS}(t+1) - P_{CS}(t)] \quad (1)$$

where $P_{CS}(t+1)$ and $P_{CS}(t)$ represent the clear-sky solar power at time *t+1* and *t*, respectively; *P(t)* is the actual solar power output at time *t*; and *SPI(t)* is the solar power index at time *t*.

In this work, the clear-sky power $P_{CS}(t)$ is calculated for all test site locations following two steps. First, the standard summer atmospheric profile of temperature, pressure, and humidity without clouds is assumed. Streamer RTM [15] is employed to calculate the Earth's surface-level GHI and DNI. Second, the CEC irradiance-to-power model, which is implemented in PV-Lib, is used to calculate AC PV output from GHI and DNI. In the irradiance-to-power calculation, we assume an ambient temperature of 300 K and no wind.

C. Methodology for Determining Target Metrics

The target values of solar forecasting metrics are derived by (i) applying uniform forecasting improvements by *x%* based on the baseline forecasting; (ii) applying ramp forecasting improvements by *y%* based on the baseline forecasting; and (iii) deriving a complete set of target metrics. The values of *x%* and *y%* are determined based on the economic impacts of improved solar power forecasting (i.e., a reduction of 25% in reserve levels, which is based on a partner utility consensus).

Two types of forecasting improvements are implemented. The improvements are categorized by the appearance of large solar ramps, which are one of the biggest concerns of high-penetration solar power scenarios. First, the start and end points of all significant ramps are extracted using the swinging door algorithm (see Section II.C.1). The definition of significant ramps is based on the magnitude of solar power change. These improvements are generated through the following procedures:

- Uniform improvements of the time series excluding ramping periods: The forecast errors of the time series when there is not a significant ramp are uniformly decreased by a percentage (*x%*).
- Ramp forecasting magnitude improvements: Only significant ramps that are identified as a change greater than or equal to a threshold value (θ) are modified in the improved forecasts. The forecast errors of the time series with ramps are decreased by a percentage (*y%*).
- Ramp forecasting threshold: The ramp forecasting threshold (θ) is set as 10% of the solar power capacity in this paper.

Figure 1 illustrates the overall structure of the methodology to determine target metrics of solar forecasting.

- First, the reserve cost of the baseline solar forecasting (C_b) is calculated, and a 25% reduction is assumed for the target reserve level (C_t).
- Second, a set of (N) combinations of *x%* uniform forecasting improvement and *y%* ramp forecasting magnitude improvements are applied to the baseline forecasting. The reserve costs (C_i) from the N improved solar forecasting combinations are calculated.
- The set of *x%* and *y%* values, with the smallest difference between the ideal target reserve cost (C_t) and the reserve cost from the improved solar forecasting (C_i), is then selected for deriving the final target value for the solar forecasting. It is important to note that other sets of *x%* and *y%* combinations can also be used if the selection criterion is changed.
- Finally, a complete set of target metrics is calculated based on the target solar forecasting value.

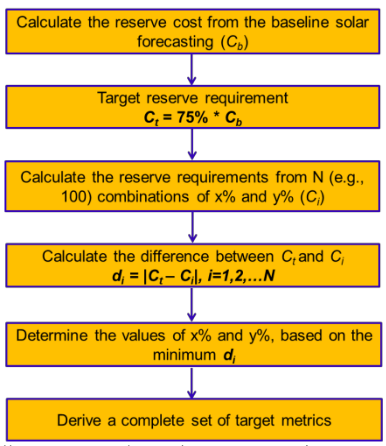

Figure 1. Overall structure to determine target metrics

1) Swinging Door Algorithm

The swinging door algorithm extracts ramp periods in a series of power signals by identifying the start and end points of each ramp. The algorithm allows for the consideration of a threshold parameter influencing its sensitivity to ramp variations. The only tunable parameter in the algorithm is the width of a "door," represented by ε. The parameter ε directly characterizes the threshold sensitivity to noise and/or insignificant fluctuations. With a smaller ε value, many small ramps will be identified; with a larger ε value, only a few large ramps will be identified. A detailed description of the swinging door algorithm can be found in [11].

2) Flexibility Reserves for 15MA, 1HA, 4HA, and DA Forecasting

The reduction in the amount of reserves that must be carried to accommodate the uncertainty of solar power output is anticipated to be one of the largest cost savings. An advanced reserve calculation algorithm is thus applied to estimate the reserve reductions that various solar power forecasting improvements would allow. This methodology was originally developed during the Western Wind and Solar Integration Study Phase 2 [16]. Improved forecasting (on average) reduces the amount of reserves that must be held, and various types of flexibility reserves are defined by:

- For 15MA, 1HA, and 4HA solar power forecasting, spinning reserves are used to derive the target solar forecasting values. Spinning reserves represent the online capacity that can be deployed very quickly (seconds to minutes) to respond to variability. In this study, the spinning reserve for 0- to 4-hours-ahead forecasting (R_s^{HA}) is defined as the 95% confidence interval ($\emptyset_{95}$) of solar power forecast errors (e^{HA}) at the 15MA, 1HA, or 4HA horizon.

$$R_s^{HA} = \emptyset_{95}(e^{HA}) \quad (2)$$

- For DA solar forecasting, both spinning and non-spinning reserves are used to derive the solar forecasting target. Non-spinning reserves represent the off-line or reserved capacity, or load resources (interruptible loads), capable of deploying within 30 minutes for at least 1 hour. In this paper, the spinning reserve for the DA forecasting (R_s^{DA}) is defined as the 70% confidence interval ($\emptyset_{70}$) of the DA solar power forecast errors (e^{DA}). The non-spinning reserve (R_{ns}^{DA}) is defined by the difference between the 95% confidence interval ($\emptyset_{95}$) and the 70% confidence interval ($\emptyset_{70}$) of the DA solar power forecast errors (e^{DA}).

$$R_s^{DA} = \emptyset_{70}(e^{DA}) \quad (3)$$

$$R_{ns}^{DA} = \emptyset_{95}(e^{DA}) - \emptyset_{70}(e^{DA}) \quad (4)$$

Considering the cost of holding and deploying reserves, this study assumes that the cost of non-spinning reserve per MW (C_{ns}^{MW}) is twice the cost of spinning reserve per MW (C_s^{MW}):

$$C_{ns}^{MW} = 2 \times C_s^{MW} \quad (5)$$

Equation (5) is derived based on the (i) start costs of multiple types of generators used for spinning and non-spinning reserves (gas turbine or oil turbine) and (ii) heat rates and fuel costs of multiple fuel types (e.g., biomass, nuclear, coal, and combined cycle).

III. CASE STUDY

Currently, there are two main customers for solar forecasting technologies: utility companies and independent system operators (ISOs). As solar penetration increases, solar forecasting will become more important to solar energy producers and solar power plant developers.

From the spatial point of view, there are two distinct types of test cases for the baseline and target values: point (single PV plant) and regional. In the point case, we are able to gather detailed information about the operational configuration of a particular PV plant (e.g., PV panel and inverter types). In conjunction with atmospheric estimates throughout the plant, we can perform physics-based numerical forecasts of the power production at the plant. We can also validate the point forecasts by using the observed power production. In the regional case, it is infeasible to gather the operational configurations for the multitude of solar PV producers in the region; however, an empirical relationship between the regional power production and the solar irradiance fields can be estimated by NWPs.

Three PV plants were chosen among hundreds of sites available by the solar utilities in the Watt-sun [17] research consortium as point test cases: Smyrna, Green Mountain Power, and Tucson Electric Power. The selection was based on the best quality, continuity, and variety of power production observations at the sites. In addition, two regional test cases were chosen to cover two distinct atmospheric conditions: a cloudier and more humid climate for the ISO-NE region in contrast to a relatively drier climate and less clouds in the CAISO region. A few assumptions were made: (i) data points at nighttime were removed when the actual or forecasted power was zero; (ii) hourly point forecasts were used for DA, 4HA, and 1HA forecasts; and (iii) 15-minute average forecasts were used for 15MA forecasts. Considering the space limitations, only the results for the CAISO case are presented in this paper.

A. Baseline Values and Target Metrics for CAISO

CAISO has 4,173 MW generation capacity distributed along the coast of California with a few large plants (20 to 40 MW) and a distribution of small (10-kW) residential and commercial installations. Concentrations are high from San Diego to Los Angeles and in San Francisco. Many larger (MW-size) plants are located in the interior of the state. Data is available in 1-hour intervals in AC production summed throughout the CAISO region. Day-to-day variations in production are relatively small.

Table 3 lists the amounts of the baseline and target reserves for different forecast horizons. For DA forecasts, the uniform forecasting improvement and ramp forecasting improvement were determined based on the combined reduction (25%) in spinning and non-spinning reserves costs. For the 15MA, 1HA, and 4HA forecasts, the improvements were determined based only on spinning reserves.

Table 3. BASELINE AND TARGET RESERVES VALUES

Forecast Horizon	Baseline Reserve (MW)	Uniform Improvement	Ramping Improvement	Target Reserve (MW)
0-23 DA spin	227.75	25.13%	30.88%	168.17
0-23 DA non-spin	448.25			335.48
24-47 DA spin	222.57	17.58%	34.83%	165.28
24-47 DA non-spin	383.46			285.49
1HA spin	459.45	25.84%	21.53%	344.68
4HA spin	766.47	37.34%	10.03%	577.69
15MA spin	111.89	40.58%	11.83%	83.96

Figure 2(a) and 3(b) illustrate the distributions of solar power forecast errors for the baseline and target forecasting, respectively. It is observed that (i) the 15MA forecasts perform the best among all forecast horizons, as shown by the peak of the distribution, and (ii) the distribution of the target forecast errors is relatively skinnier than the corresponding distribution of the baseline forecast errors.

The baseline values and target metrics are summarized in Table 4. The NAM model for the DA forecasts and the persistence model for the 4HA, 1HA, and 15MA forecasts are accurate with very high correlation coefficients and small RMSE and MAPE values. The relatively larger RMSE and MAE values in the 4HA forecasts are partially attributed to the inherent assumption that indirect light and panel temperature changes of more than 4 hours are not accounted for. The financial baseline and targets can be translated back to forecasting accuracy metrics and requirements, which will guide research on solar forecasting improvements towards the areas that are most beneficial to power systems operations.

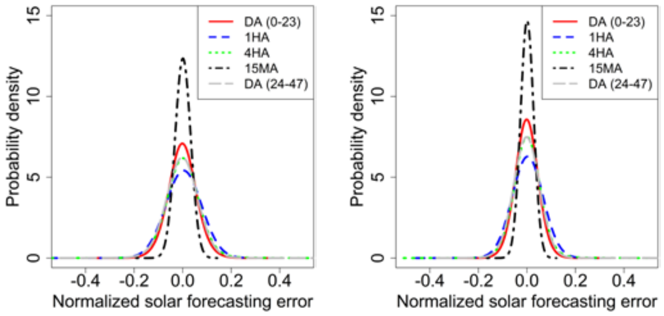

(a) Baseline (b) Target

Figure 2. Distribution of baseline values and target metrics for solar power forecast errors at DA, 4HA, 1HA, and 15MA forecast horizons

Table 4. Baseline Values and Target Metrics for CAISO at Different Forecast Horizons

Metrics	DA (24-47) Baseline	DA (24-47) Target	DA (0-23) Baseline	DA (0-23) Target	4HA Baseline	4HA Target	1HA Baseline	1HA Target	15MA Baseline	15MA Target
Correlation coefficient	0.97	0.98	0.98	0.99	0.96	0.97	0.98	0.99	1.00	1.00
RMSE (MW)	168.39	120.05	150.54	110.82	184.62	149.17	119.91	90.75	29.01	21.42
NRMSE by capacity	0.04	0.03	0.04	0.03	0.04	0.04	0.03	0.02	0.01	0.01
MaxAE (MW)	2728.00	1777.89	860.02	619.10	1736.00	1561.86	1252.63	982.93	313.16	276.12
MAE (MW)	98.56	71.74	98.91	72.68	111.97	85.35	93.98	70.95	22.24	15.45
MAPE by capacity	0.02	0.02	0.02	0.02	0.03	0.02	0.02	0.02	0.01	0.00
MBE (MW)	-8.25	-6.55	-5.72	-4.46	4.45	4.38	16.74	12.42	4.43	3.35
KSIPer (%)	16.61	14.12	16.36	14.71	31.02	22.68	38.91	31.88	16.93	13.82
OVERPer (%)	0.00	0.00	0.00	0.00	0.00	0.00	0.08	0.00	0.00	0.00
Standard dev. (MW)	168.25	119.92	150.47	110.76	184.63	149.16	118.77	89.91	28.68	21.16
Skewness	3.04	2.30	0.04	0.04	0.83	1.02	-0.40	-0.49	-0.42	-0.64
Kurtosis	59.89	43.03	3.17	3.15	13.27	19.81	5.86	6.74	6.42	13.96
4RMQE (MW)	472.71	311.54	237.20	174.47	371.25	326.40	204.29	158.20	50.08	42.77
N4RMQE by capacity	0.11	0.07	0.06	0.04	0.09	0.08	0.05	0.04	0.01	0.01
95th percentile (MW)	304.10	227.02	339.69	251.51	386.30	298.80	229.08	175.52	55.85	42.29
Renyi entropy	3.09	3.24	4.21	4.23	3.44	3.13	4.54	4.51	4.42	4.07
NRMSE by clear-sky power	0.31	0.22	0.26	0.19	0.27	0.22	0.19	0.14	0.02	0.02
MAPE by clear-sky power	0.18	0.13	0.17	0.13	0.16	0.12	0.15	0.11	0.02	0.01

IV. CONCLUSION

To conclude, we note that the development of baseline and target values for solar forecasting is closely related to the objective of quantifying the economic benefit of solar forecasting, around which currently the industry has no consensus. This is not only because of the complicated hierarchy and structure of the electrical energy market, but also because of the lack of in-depth understanding about how the forecast information may seamlessly fit into utility or ISO operations. Our development of baseline values and target economic metrics for quantifying the benefits of the solar forecast system has been based on close collaboration with utility and ISO partners.

As a result of such communications with utilities and ISOs, we found that although solar forecasts are likely to have a multitude of economic benefits, the industry agrees that improved solar forecast accuracy will lead to a reduction in the amount of minimum reserves that must be carried to accommodate the uncertainty of solar power output. Such a reduction in reserves is likely to be one of the largest cost savings in the near future. Toward this end, we have provided the actual amount of reduction in spinning and non-spinning reserves for the test case, after the forecast accuracy is improved from the baseline to the target value. From these results, we note that even at present, the amount of reserve reduction for CAISO will be several hundred MW, which will correspond to an annual savings on the order of $100 million. The savings will continue to grow in the next years as the level of PV power penetration increases in the region.

REFERENCES

[1] R. Margolis, C. Coggeshall, and J. Zuboy, J., "SunShot vision study," U.S. Department of Energy, Washington, D.C., 2012.

[2] M. Diagne, M. David, P. Lauret, J. Boland, and N. Schmutz, "Review of solar irradiance forecasting methods and a proposition for small-scale insular grids," *Renewable and Sustainable Energy Reviews*, vol. 27, pp. 65-76, 2013.

[3] International Energy Agency, "Photovoltaic and solar forecasting: State of the art," Paris, France, Tech. Rep. IEA PVPS T14-01:2013, 2013.

[4] R. Perez, S. Kivalov, J. Schlemmer, K. Hemker, D. Renne, and T. E. Hoff, "Validation of short and medium term operational solar radiation forecasts in the U.S.," *Solar Energy*, vol. 84, no. 12, pp. 2161-2172, 2010.

[5] R. Perez, et al., "Comparison of numerical weather prediction solar irradiance forecasts in the US, Canada and Europe," *Solar Energy*, vol. 94, pp. 305-326, 2013.

[6] E. Lorenz et al., "Benchmarking of different approaches to forecast solar irradiance," in *Proc. 24th European Photovoltaic Solar Energy Conf.*, pp. 4199-4208, 2009.

[7] P. Mathiesen, and J. Kleissl, "Evaluation of numerical weather prediction for intra-day solar forecasting in the continental United States," *Solar Energy*, vol. 85, no. 5, pp. 967-977, 2011.

[8] E. Lorenz, T. Scheidsteger, J. Hurka, D. Heinemann, and C. Kurz, "Regional PV power prediction for improved grid integration," *Progress in Photovoltaics: Research and Applications*, vol. 19, no. 7, pp. 757-771, 2011.

[9] E. Lorenz, D. Heinemann, and C. Kurz, "Local and regional photovoltaic power prediction for large scale grid integration: Assessment of a new algorithm for snow detection," *Progress in Photovoltaics: Research and Applications*, vol. 20, no. 6, pp. 760-769, 2012.

[10] M. Paulescu, E. Paulescu, P. Gravila, and V. Badescu, *Weather Modeling and Forecasting of PV Systems Operation*, Springer, London, 2013.

[11] J. Zhang, A. Florita, B.-M. Hodge, S. Lu, H. F. Hamann, V. Banunarayanan, and A. M. Brockway, "A suite of metrics for assessing the performance of solar power forecasting," *Solar Energy* (in press).

[12] U. Germann, I. Zawadzki, and B. Turner, "Predictability of precipitation from continental radar images Part IV: limits to prediction," *Journal of the Atmospheric Sciences*, vol. 63, no. 8, pp. 2092-2108, 2006.

[13] F. Mesinger et al., "North American regional reanalysis," *Bulletin of the American Meteorological Society*, vol. 87, no. 3, pp. 343–360, 2006.

[14] J. S. Stein, "The photovoltaic performance modeling collaborative (PVPMC)," in *Proc. 38th IEEE Photovoltaic Specialists Conference*, Austin, Texas, 2012.

[15] J. Key and A. J. Schweiger, "Tools for atmospheric radiative transfer: Streamer and FluxNet," *Computers and Geosciences*, vol. 24, no. 5, pp. 443-451, 1998.

[16] D. Lew et al., "The western wind and solar integration study phase 2," National Renewable Energy Laboratory, Golden, CO, Tech. Rep. NREL/TP-5500-55888, 2013.

[17] S. Lu et al., "A multi-scale solar energy forecast platform based on machine-learned adaptive combination of expert systems," in *Proc. 94th American Meteorological Society Annual Meeting*, Atlanta, GA, 2014.